Circuits, Systems, and Signal Processing (2024) 43:5507–5531
https://doi.org/10.1007/s00034-024-02714-1

The Second-Order Sliding Mode Control Algorithm for Fixed-Time Stability of Nonlinear Systems

Qinjun Zeng[1] · Minghui Jiang[1] · Junhao Hu[2]

Received: 6 November 2023 / Revised: 25 April 2024 / Accepted: 26 April 2024 /
Published online: 20 May 2024

Abstract

This article focuses on the fixed-time stability of a class of nonlinear systems with uncertain disturbances and time-varying delays. Different from other papers, the second-order sliding mode control algorithm (SOSMCA) is developed in this article to study the fixed-time stability of nonlinear systems for the first time. Additionally, the novel sliding mode surface (SMC) and second-order SMC are presented. And the stability and reachability of the sliding-mode dynamics under a faster settling time are demonstrated. Finally, the applicability and validity of the obtained SOSMCA are demonstrated by a simulation example with the F-404 aircraft engine model.

Keywords Nonlinear systems · Second-order sliding mode control · Fixed-time stability · Sliding mode surface

1 Introduction

A variety of dynamical systems can be modeled using equations based on linearity. Nevertheless, it frequently runs into the problem that the linear framework is inadequate or erroneous for analyzing dynamical systems. Naturally, non-linear systems (NSs) are employed to characterize this type of dynamical system [33]. To date, the controlling of NSs has attracted significant concern from investigators on account of the wide range of applications they have in a variety of domains, including neural net-

✉ Minghui Jiang
jiangminghui@ctgu.edu.cn

Qinjun Zeng
3097517851@qq.com

Junhao Hu
junhaohu74@163.com

1 Institute of Nonlinear Complex Systems, China Three Gorges University, Yi Chang 443000, Hubei, China

2 College of Mathematics and Statistics, South Central University for Nationalities, Wuhan 430074, Hubei, China

works [35], repetitive control systems [52, 53], offshore platforms [44, 46], industrial manipulator [26], Kuramoto-oscillator systems [29], and bioreactors [8]. Meanwhile, several kinds of NSs have been thoroughly studied [3, 28, 30, 45], such as switched NSs, stochastic NSs, uncertain NSs, and others.

The stability, robustness, and performance of the actual systems tend to be damaged by uncertainties introduced to them. To fight off structural disturbances and uncertainties, investigators adopt sliding mode control (SMC) owing to its robust performance or unchanging behavior property. On the other hand, it is a reality that we usually ask for error convergence within a finite time for nonlinear systems. Until now, numerous findings have been made regarding the finite-time control of nonlinear systems, but they still have certain limitations. For example, the time delay is not considered for non-linear systems containing complete state restrictions in some works [36, 40, 45]. In the works [18, 22, 49], the controller makes use of the bound of uncertainty. In [6, 38], intergral sliding surfaces to support SMC are employed. Recently, a number of additional articles have focused on this topic, just as noted in [12, 47, 48]. The writers in [47, 48] impliedly used the disturbance's bounds, and this reflects the shortcoming in their efforts. Also, the simulation work results from [12] demonstrate that the approach they recommend performs not very well. Another piece of work described in [42] focuses on the strategies for control associated with quadrotor dynamics involving time-varying disturbances as well as unidentified dynamics, where the terminal sliding method is the foundation of the proposed strategy. Some papers, including [10, 51], are concerned with linear systems. In [10], an approach based on LMI is presented for linear systems. From another perspective, none of the above works considered the fixed-time control issue associated with nonlinear systems, which is a great pity.

Unfortunately, one critical shortcoming of SMC is chattering, which is characterized by little-amplitude oscillations with finite as well as high frequencies. Chattering could cause certain damage to the mechanical or electrical components of systems. However, the majority of the literature ignores this problem. For example, the chattering is not taken away since the sign function is straight away built into the input signal for control [11, 14, 50]. In addition, although the adaptive control law is applied in the controller in [54], the controller still contains the sign function, which leads to the chattering. To address this issue, A. Levant put forward the idea of "sliding order" and offered a number of second-order sliding mode (SOSM) control strategies [2]. In contrast to the first-order SMC algorithms, the SOSM control technology not only broadens the benefits of conventional SMC to systems with greater relative degrees successfully but can also be utilized to reduce chattering effects and increase control precision [15]. So far, remarkable advances in SOSM control have been made [4, 5, 19, 25, 34]. However, the closed-loop systems' convergence at a fixed time cannot be guaranteed by the proposed SOSM controller [5, 19]. In [4, 25], the authors did not consider the impact of the time delay, which constitutes a limitation in their works. In [34], the restriction on the bound of the perturbation derivative is relaxed to be unbounded; however, the proposed control input with discontinuity causes the chattering.

Inspired by the discussion above, this study will concentrate on SOSM control for the fixed-time stability of nonlinear systems in the face of uncertain disturbances and time-varying delays. The following are the key novelties of our contribution:

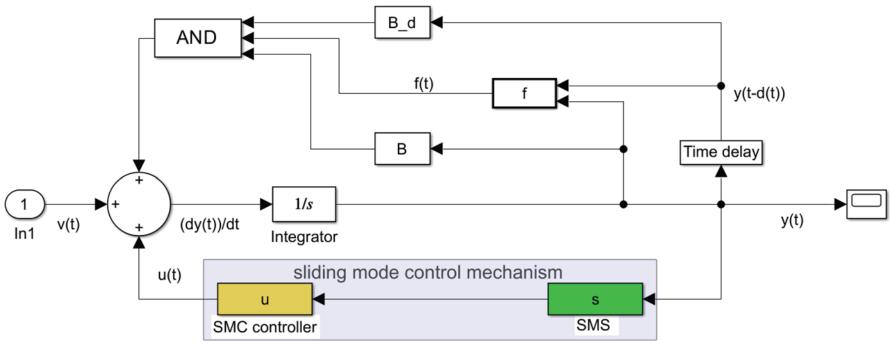

Fig. 1 Block diagram of SOSM control for the non-linear system with uncertain disturbances and time-varying delays

(1) A new fixed-time control scheme combined with second-order SMC is put forward to stabilize a class of nonlinear systems containing uncertain disturbances as well as time-varying delays.
(2) The real, predetermined settling time of sliding modules that meet performance requirements can be adjusted in advance in the most direct way.
(3) With the increase in sliding mode order, the magnitude of chattering is diminished, and the precision of control is enhanced.

Notations: $\Re_+, \Re^p$, and $\Re^{p\times p}$ represent the positive real number, real vector of dimension p, and real square matrix of dimension p, respectively. Define the upper right-hand Dini derivative of a continuous function as follows: $D^+V(t) = \lim_{h\to+0}\sup\frac{V(t+h)-V(t)}{h}$.

2 Model Description and Preliminaries

As shown in the block diagram in Fig. 1, a nonlinear system under sliding mode control is represented as follows, where external disturbances and time-varying delays are included to extend the generality of the system.

$$\begin{aligned}\dot{y}(t) =& By(t) + B_d y(t-d(t)) + \pounds(t, y(t), y(t-d(t)) + v(t) + u(t),\\ y(t) =& \varkappa(t), \forall t \in [-\hbar, 0],\end{aligned} \tag{1}$$

where $y(t) \in \Re^p$ is the system's state. $B \in \Re^{p\times p}$ and $B_d \in \Re^{p\times p}$ denote constant matrices. $\pounds(\cdot) \in \Re^p$ represents the non-linear function. $v(t) \in \Re^p$ is the uncertain disturbance. $u(t) \in \Re^p$ represents the input signal. $d(t)$ represents the time-varying delay satisfying the condition listed below:

$$0 \le d(t) \le \hbar \text{ for the real constant } \hbar > 0,\ \dot{d}(t)\ exists. \tag{2}$$

$\varkappa(t)$ corresponds to the initial value on $[-\hbar, 0]$.

Remark 1 To infer the stability of time-delay systems with Lyapunov stability theory, it is crucial to comprehend the derivative information of the delay [9]. However, the assumption with respect to it is restricted in the documents [16, 27, 37, 43], where [16, 37, 43] require the derivative of the delay to be less than 1 and [27] requires the derivative of the delay to be bounded, all of which require the existence of an upper bound for the derivative. Unlike these documents, the more general and valid hypothesis (2) is given, in which the derivative of the delay is relaxed to unbounded. This allows our results to be applied more widely.

Let $£(t, y(t), y(t-d(t))) = £(t)$ for convenience, system (1) is therefore represented as

$$\begin{aligned} \dot{y}(t) =& By(t) + B_d y(t-d(t)) + £(t) + v(t) + u(t), \\ y(t) =& \varkappa(t), \forall t \in [-\hbar, 0], \end{aligned} \tag{3}$$

which is transformed to be

$$\begin{aligned} \dot{y}_\ell(t) =& B_\ell y(t) + B_{d\ell} y(t-d(t)) + £_\ell(t) + v_\ell(t) + u_\ell(t), \\ y_\ell(t) =& \varkappa_\ell(t), \quad \forall t \in [-\hbar, 0], \quad \ell = 1, 2, \ldots, p, \end{aligned} \tag{4}$$

in which $y_\ell(t)$ corresponds to the ℓth element in vector $y(t)$. B_ℓ and $B_{d\ell}$ denote the ℓth row of matrices $B,\ B_d$, respectively. $£_\ell(t),\ v_\ell(t),$ and $u_\ell(t)$, respectively, denote the ℓth element in vectors $£(t),\ v(t),\ and\ u(t)$.

Assumption 1 The uncertain disturbance vector $v(t)$ fulfills

$$|\dot{v}_\ell(t)| \leq \delta_\ell,$$

in which $\delta_\ell > 0,\ \ell = 1, 2, \ldots, p$, are known constants representing the boundedness of the uncertain of system (1).

Definition 1 ([14, 24]) The system (1) is deemed to be globally finite-time stable once any solution $y(t, y_0)$ reaches its equilibria in finite time, namely, $y(t, y_0) = 0,$ for $t > \urcorner(y_0),\ y_0 \in \Re^p$ in which $\urcorner : \Re^p \to \Re_+ \cup \{0\}$ is referred to as the settling-time function.

For instance, any solution $y(y_0)$ to the system

$$\dot{y} = -y^{1/3}, y \in \Re$$

arrives at the zero equilibrium point in the finite period $\urcorner(y_0) := \frac{3}{2}\sqrt[3]{|y_0|^2}$.

Definition 2 ([14, 24]) System (1) is deemed to be globally fixed-time stable once the settling-time function $\urcorner(y_0)$ is bounded, namely, $\exists \urcorner_{max} > 0 : \urcorner(y_0) \leq \urcorner_{max}, \forall\, y_0 \in \Re^p$.

For example, the zero equilibrium of the system

$$\dot{y} = -y^{1/3} - y^3, y \in \Re,$$

is stable in a fixed period with the settling-time function satisfying $\daleth(y_0) \leq 2.5, \forall y_0 \in \Re$.

Remark 2 To obtain the stability of the nonlinear system (1) in a fixed period through sliding mode control, it's necessary to transform system (1) to system (4). Additionally, a single equilibrium point (or simple solution) $y(t, \varkappa(t))$ of system (1) could be verified in accordance with [9, 17] if Assumption 1 is satisfied.

This paper focuses on the following issue:

developing a feedback controller $u = u(y)$ that ensures the fixed-time stability of the system (1) for a specified global settling-time estimate $\daleth_{max}$.

3 Retrofit Fixed-Time Stability Theorem

Before developing a SOSM controller, we first give the following novel fixed-time theorem:

Theorem 1 *Take into account the non-negative scalar system*

$$\dot{y} = -(a_0 y^{\alpha} + b_0 y^{\beta})^{\gamma}, \ \ y(0) = y_0, \tag{5}$$

where $a_0, b_0, \alpha, \beta, \gamma$ are positive numbers satisfying $\alpha\gamma < 1, \ \beta\gamma > 1$. Then, System (5) is globally stable in a fixed time, with the upper bound on the settling period determined as

$$\daleth(y_0) < b_0^{-\gamma} \left(\frac{a_0}{b_0}\right)^{\frac{1-\beta\gamma}{\beta-\alpha}} \left(\frac{1}{1-\alpha\gamma} + \frac{1}{\beta\gamma - 1}\right). \tag{6}$$

Proof Suppose $\mathscr{C}(y) = y^2 \geq 0$. Then, the differentiation of $\mathscr{C}(y)$ along system (5) is

$$\dot{\mathscr{C}}(y) = -2y\left(a_0 y^{\alpha} + b_0 y^{\beta}\right)^{\gamma} = -2(\mathscr{C}(y))^{\frac{1}{2}}\left(a_0(\mathscr{C}(y))^{\frac{\alpha}{2}} + b_0(\mathscr{C}(y))^{\frac{\beta}{2}}\right)^{\gamma}.$$

For $\mathscr{C}(y) \neq 0$, we have

$$\frac{\frac{1}{2}\mathscr{C}^{-\frac{1}{2}} d\mathscr{C}}{\left(a_0 \mathscr{C}^{\frac{\alpha}{2}} + b_0 \mathscr{C}^{\frac{\beta}{2}}\right)^{\gamma}} = -dt. \tag{7}$$

Let $z = \mathscr{C}^{\frac{1}{2}}$, Eq. (7) could be rewritten as

$$\frac{dz}{\left(a_0 z^{\alpha} + b_0 z^{\beta}\right)^{\gamma}} = -dt. \tag{8}$$

From the differential formula and the definition of z, Eq. (8) yields

$$d\left(\int_0^z \frac{1}{\left(a_0 \tau^{\alpha} + b_0 \tau^{\beta}\right)^{\gamma}} d\tau\right) = \frac{1}{\left(a_0 z^{\alpha} + b_0 z^{\beta}\right)^{\gamma}} dz = -dt.$$

Integrate each side of the aforementioned formula from 0 to t and consider $z = \mathscr{C}^{\frac{1}{2}}$,

$$\int_0^{z(t)} \frac{1}{\left(a_0\tau^\alpha + b_0\tau^\beta\right)^\gamma} d\tau = \int_0^{z(0)} \frac{1}{\left(a_0\tau^\alpha + b_0\tau^\beta\right)^\gamma} d\tau - \int_0^t d\tau. \tag{9}$$

Since $z = 0$ could be guaranteed as if $\int_0^{z(t)} \frac{1}{\left(a_0\tau^\alpha + b_0\tau^\beta\right)^\gamma} d\tau = 0$, the following settling-time function is determined according to Eq. (9)

$$\begin{aligned} \urcorner(y_0) &= \int_0^{z(0)} \frac{1}{\left(a_0\tau^\alpha + b_0\tau^\beta\right)^\gamma} d\tau \\ &= \int_0^{k} \frac{1}{\left(a_0\tau^\alpha + b_0\tau^\beta\right)^\gamma} d\tau + \int_k^{z(0)} \frac{1}{\left(a_0\tau^\alpha + b_0\tau^\beta\right)^\gamma} d\tau \\ &\le \int_0^{k} \frac{1}{a_0^\gamma \tau^{\alpha\gamma}} d\tau + \int_k^{+\infty} \frac{1}{b_0^\gamma \tau^{\beta\gamma}} d\tau = \frac{k^{1-\alpha\gamma}}{(1-\alpha\gamma)a_0^\gamma} + \frac{k^{1-\beta\gamma}}{(\beta\gamma-1)b_0^\gamma} \end{aligned} \tag{10}$$

where k is a non-negative real number. Define the function $h(\cdot) = \frac{k^{1-\alpha\gamma}}{(1-\alpha\gamma)a_0^\gamma} + \frac{k^{1-\beta\gamma}}{(\beta\gamma-1)b_0^\gamma}$ with the variable k. Take the derivative of $h(\cdot)$, one knows:

$$\begin{aligned} \frac{d(h)}{d(k)} &= \frac{k^{-\alpha\gamma}}{a_0^\gamma} - \frac{k^{-\beta\gamma}}{b_0^\gamma} = \frac{b_0^\gamma k^{-\alpha\gamma} - a_0^\gamma k^{-\beta\gamma}}{(a_0 b_0)^\gamma} \\ &\Longrightarrow \frac{d(h)}{d(k)} = 0,\ when\ k = \left(\frac{a_0}{b_0}\right)^{\frac{1}{\beta-\alpha}}. \end{aligned}$$

Since $\lim_{k\to 0} h(\cdot) = \lim_{k\to+\infty} h(\cdot) = +\infty$, the function $h(\cdot)$ has a minimum value at $k = \left(\frac{a_0}{b_0}\right)^{\frac{1}{\beta-\alpha}}$, which is

$$\frac{a_0^{\frac{1-\beta\gamma}{\beta-\alpha}}}{b_0^{\frac{1-\alpha\gamma}{\beta-\alpha}}}\left(\frac{1}{1-\alpha\gamma} + \frac{1}{\beta\gamma-1}\right) = b_0^{-\gamma}\left(\frac{a_0}{b_0}\right)^{\frac{1-\beta\gamma}{\beta-\alpha}}\left(\frac{1}{1-\alpha\gamma} + \frac{1}{\beta\gamma-1}\right).$$

Based on (10), there is

$$\urcorner(y_0) \le inf\,\{h(\cdot)\} = min\,\{h(\cdot)\}\,. \tag{11}$$

The evidence is finished. □

Remark 3 This note will emphasize the advantages of Theorem 1. Consider the classical works [13, 24, 34], where the global settling-time estimate for system (5) takes the following size:

$$\daleth(y_0) \leq \frac{1}{(1-\alpha\gamma)a_0^{\gamma}} + \frac{1}{(\beta\gamma-1)b_0^{\gamma}} \quad for \ \ \forall y_0 \in \Re. \tag{12}$$

Note that it is a more conservative upper-bound calculation than inequality (6). This is because the value of its right end equals to $h(k)\big|_{k=1}$, which is bigger than the right end in (6)(based on the inequality (11)). On the other hand, the system (5) turns into the widely studied and applied system model in [21, 31, 41, 55] when $\gamma = 1$. They give the following best-known estimate for the settlement time of this system:

$$\daleth(y_0) \leq \frac{1}{(1-\alpha)a_0} + \frac{1}{(\beta-1)b_0} \quad for \ \ \forall y_0 \in \Re, \ \gamma = 1.$$

Also, it is a special case of the right side of (12). Overall, the inequality (6) expands the existing research [13, 21, 24, 31, 34, 41, 55] by providing a faster estimate for the rate of convergence.

4 Second-Order Integral Sliding Mode Control

The contents of this section are separated as follows: In Sect. 4.1, a SOSM controller is designed. In Part 4.2, the fixed-time stability of SMS is demonstrated. In Part 4.3, it is proved that the system (4) will first reach the second-order SMS $\varrho_\ell(t) = 0$ in a fixed period and then slide to the SMS $\varpi_\ell(t) = 0$ in a fixed period.

For simplicity, the following notations that will be used later is first given:

$$\beth^{[m]} = |\beth|^m sign(\beth), \; F(\beth) = e^{|\beth|}, \; \beth \in \Re, m \in \Re_+$$

which present the involution process without the sign of the number being lost and the compound function with the even function property, respectively. For any $\beth \in \Re, r, \ m \in \Re_+$, the following properties hold:

$$\begin{aligned} &i). \ (-\beth)^{[m]} = -\beth^{[m]}, \\ &ii). \ \left(\beth^{[m]}\right)^{[r]} = \left(\beth^{[r]}\right)^{[m]}, \\ &iii). \ \int_0^{+\infty} \frac{1}{F(t)} dt = 1. \end{aligned} \tag{13}$$

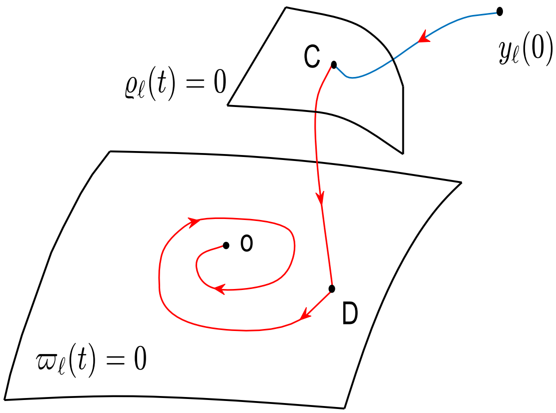

Fig. 2 Two stages of the second-order SMC

Proof Based on the definition of the symbols $[\cdot]$ and $F(\cdot)$, properties 1 and 3 are obvious. On the other hand,

$$\begin{aligned} ii).\left(\gimel^{[m]}\right)^{[r]} &= \left|\gimel^{[m]}\right|^{r} sign(\gimel^{[m]}) = \left(|\gimel|^{m}\right)^{r} sign(\gimel) = \left(|\gimel|^{r}\right)^{m} sign(\gimel) \\ &= \left|\gimel^{[r]}\right|^{m} sign(\gimel^{[r]}) \\ &= \left(\gimel^{[r]}\right)^{[m]}. \end{aligned} \tag{14}$$

The proof is finished. □

Remark 4 The goal of SMC is to implement sliding-mode motion in the system. Additionally, the sliding action completely determines how the system behaves. The arriving stage ($y_\ell(0) \dashrightarrow C$) and the sliding stage ($C \dashrightarrow D \dashrightarrow o$) make up the second-order SMC's whole control process (refer to Fig. 2).

4.1 SMS Design

The sliding mode surface (SMS) designed in this study is as follows:

$$\varpi_\ell(t) = y_\ell(t) + \frac{r_\ell}{\daleth_\ell^s m_\ell} \int_0^t y_\ell^{[1-\frac{m_\ell}{r_\ell}]}(\curlywedge) F\left(y_\ell^{[\frac{m_\ell}{r_\ell}]}(\curlywedge)\right) d\curlywedge, \tag{15}$$

where the sclar $\daleth_\ell^s > 0, r_\ell$ and m_ℓ are positive integers satisfying $0 < \frac{m_\ell}{r_\ell} < 1,$ and $\ell = 1, \ldots, p.$

The derivative of $\varpi_\ell(t)$ with regard to t is

$$\dot{\varpi}_\ell(t) = \dot{y}_\ell(t) + \frac{r_\ell}{\daleth_\ell^s m_\ell} y_\ell^{[1-\frac{m_\ell}{r_\ell}]}(t) F\left(y_\ell^{[\frac{m_\ell}{r_\ell}]}(t)\right). \tag{16}$$

Replace $\dot{y}_\ell(t)$ with the right band of (4) to get

$$\dot{\varpi}_\ell(t) = B_\ell y(t) + B_{d\ell} y(t - d(t)) + £_\ell(t) + v_\ell(t) + u_\ell(t) + \frac{r_\ell}{\daleth_\ell^s m_\ell} y_\ell^{[1-\frac{m_\ell}{r_\ell}]}(t) F\Big(y_\ell^{[\frac{m_\ell}{r_\ell}]}(t)\Big). \tag{17}$$

Construct the following second-order SMS utilizing $\varpi_\ell(t)$ and $\dot{\varpi}_\ell(t)$

$$\varrho_\ell(t) = \dot{\varpi}_\ell(t) + \frac{1}{\daleth_\ell^r}\Big(\big(\daleth_\ell^r\big)^2 \dot{\varpi}_\ell^{[2]}(t) + 72 sign(\varpi_\ell(t)) + 72\varpi_\ell^{[3]}(t)\Big)^{[\frac{1}{2}]} \tag{18}$$

where $\daleth_\ell^r$ is a positive sclar.
Set up the controller $u_\ell(t)$ as shown below:

$$\begin{aligned} u_\ell(t) = &-B_\ell y(t) - B_{d\ell} y(t - d(t)) - £_\ell(t) - \frac{r_\ell}{\daleth_\ell^s m_\ell} y_\ell^{[1-\frac{m_\ell}{r_\ell}]}(t) F\Big(y_\ell^{[\frac{m_\ell}{r_\ell}]}(t)\Big) \\ &- \int_0^t \Big(\frac{108}{(\daleth_\ell^r)^2}\varpi_\ell^2(人) sign(\varrho_\ell(人)) + \delta_\ell sign(\varrho_\ell(人)) \\ &+ \frac{2\pi}{\daleth_\ell^r}\Big(\varrho_\ell^{[\frac{1}{2}]}(人) + \varrho_\ell^{[\frac{3}{2}]}(人)\Big)^{[1]}\Big) d 人 . \end{aligned} \tag{19}$$

Substituting (19) into (4) gives the following closed-loop system:

$$\begin{aligned} \dot{y}_\ell(t) = v_\ell(t) &- \frac{r_\ell}{\daleth_\ell^s m_\ell} y_\ell^{[1-\frac{m_\ell}{r_\ell}]}(t) F\Big(y_\ell^{[\frac{m_\ell}{r_\ell}]}(t)\Big) \\ &- \int_0^t \Big(\frac{108}{(\daleth_\ell^r)^2}\varpi_\ell^2(人) sign(\varrho_\ell(人)) + \delta_\ell sign(\varrho_\ell(人)) \\ &+ \frac{2\pi}{\daleth_\ell^r}\Big(\varrho_\ell^{[\frac{1}{2}]}(人) + \varrho_\ell^{[\frac{3}{2}]}(人)\Big)^{[1]}\Big) d 人 . \end{aligned} \tag{20}$$

4.2 Stability of Sliding-Mode Dynamics

Next, the stability of sliding-mode dynamics in a fixed period will be checked in this subsection.
The following equation holds when the SMS $\varpi_\ell(t) = 0$ is reached [32]:

$$\varpi_\ell(t) = \dot{\varpi}_\ell(t) = \ddot{\varpi}_\ell(t) = 0.$$

Based on (16), the sliding-mode dynamic is thus established as

$$\dot{y}_\ell(t) = -\frac{r_\ell}{\daleth^s_\ell m_\ell} y_\ell^{[1-\frac{m_\ell}{r_\ell}]}(t) F\left(y_\ell^{[\frac{m_\ell}{r_\ell}]}(t)\right). \tag{21}$$

Theorem 2 *For $\ell = 1, \ldots, p$, the sliding mode (21) attains stability at a preset convergence time $\daleth^s_\ell$.*

Proof Choose the radially unbounded Lyaponuv function as $\mathscr{C}_1(t) = |y_\ell(t)|$ and obtain the time derivative of $\mathscr{C}_1(t)$ following the track of (21) to be:

$$\begin{aligned}\dot{\mathscr{C}}_1(t) &= \dot{y}_\ell(t) sign(y_\ell(t)) \\ &= -\frac{r_\ell}{\daleth^s_\ell m_\ell} |y_\ell(t)|^{1-\frac{m_\ell}{r_\ell}} F\left(|y_\ell(t)|^{\frac{m_\ell}{r_\ell}}\right) \\ &= -\frac{r_\ell}{\daleth^s_\ell m_\ell} \mathscr{C}_1^{1-\frac{m_\ell}{r_\ell}}(t) F\left(\mathscr{C}_1^{\frac{m_\ell}{r_\ell}}(t)\right) \leq 0.\end{aligned}$$

This guarantees that system (21) is asymptotically stable. Rewrite the above expression as

$$\frac{d\mathscr{C}_1(t)}{dt} = -\frac{r_\ell}{\daleth^s_\ell m_\ell} \mathscr{C}_1^{1-\frac{m_\ell}{r_\ell}}(t) F\left(\mathscr{C}_1^{\frac{m_\ell}{r_\ell}}(t)\right).$$

According to the above equation, we have

$$\frac{m_\ell}{r_\ell} \frac{d\mathscr{C}_1(t)}{\mathscr{C}_1^{1-\frac{m_\ell}{r_\ell}}(t) F\left(\mathscr{C}_1^{\frac{m_\ell}{r_\ell}}(t)\right)} = -\frac{1}{\daleth^s_\ell} dt.$$

This is equivalent to

$$\frac{m_\ell}{r_\ell} \frac{\mathscr{C}_1^{\frac{m_\ell}{r_\ell}-1}(t) d\mathscr{C}_1(t)}{F\left(\mathscr{C}_1^{\frac{m_\ell}{r_\ell}}(t)\right)} = -\frac{1}{\daleth^s_\ell} dt. \tag{22}$$

Denoting the new variable $\mathscr{E}(t) = \mathscr{C}_1^{\frac{m_\ell}{r_\ell}}(t)$, whose derivative with respect to $\mathscr{C}_1(t)$ is $d\mathscr{E}(t) = \frac{m_\ell}{r_\ell} \mathscr{C}_1^{\frac{m_\ell}{r_\ell}-1}(t) d\mathscr{C}_1(t)$, the following simple form can be obtained by using the variable substitution for (22):

$$\frac{d\mathscr{E}(t)}{F(\mathscr{E}(t))} = -\frac{1}{\daleth^s_\ell} dt. \tag{23}$$

Through the aid of the definition of $F(\cdot)$ and the differential formula under integral, we can know

$$d\left(\int_0^y \frac{1}{F(\curlywedge)} d\curlywedge\right) = \frac{1}{F(y)} dy. \tag{24}$$

As a consequence, Eq. (23) can be rewritten as:

$$d\Big(\int_0^{\mathscr{E}} \frac{1}{F(人)} d\,人\Big) = -\frac{1}{\daleth_\ell^s} dt.$$

For now, assume that the arrival time for the ℓth sliding module is γ^r (the existence and boundedness of the arrival time can be guaranteed from Sect. 4.3). Then, if each side of the aforementioned formula is integrated from γ^r to t while considering $\mathscr{E} = \mathscr{C}_1^{\frac{m_\ell}{r_\ell}}(t)$ and $\mathscr{C}_1 = |y_\ell(t)|$, one knows:

$$\int_0^{|y_\ell(t)|^{\frac{m_\ell}{r_\ell}}} \frac{1}{F(人)} d人 = -\frac{1}{\daleth_\ell^s}(t - \gamma^r) + \int_0^{|y_\ell(\gamma^r)|^{\frac{m_\ell}{r_\ell}}} \frac{1}{F(人)} d\,人\,.$$

Obviously, the inference that $y_\ell(t) = 0$ is true if and only if $\int_0^{|y_\ell(t)|^{\frac{m_\ell}{r_\ell}}} \frac{1}{F(人)} d人 = 0$. Consequently, the settling-time function is determined below:

$$\daleth(y_\ell(\gamma^r)) = \gamma^r + \daleth_\ell^s \int_0^{|y_\ell(\gamma^r)|^{\frac{m_\ell}{r_\ell}}} \frac{1}{F(人)} d\,人\,.$$

This derives the stability of system (21) in a finite time. In addition, it holds that $0 \le \int_0^{|y_\ell(\gamma^r)|^{\frac{m_\ell}{r_\ell}}} \frac{1}{F(人)} d人 \le 1$ in accordance with (13). Utilizing this property, there is

$$\daleth(y_\ell(\gamma^r)) \le \gamma^r + \daleth_\ell^s.$$

Thus, an upper bound for the setting-time function that is unaffected by the state value at the arrival time is established. This means that the definition of fixed-time stability for the sliding-mode dynamic (21) is satisfied. The evidence is finished. □

Remark 5 In accordance with the stability theorem in [7], the existence of $\int_0^{+\infty} \frac{1}{F(t)} dt$ is one sufficient condition for the fixed-time stability of the SMS (15). To satisfy this condition, the $F(t)$ that occurred in the existing research [14, 43] was respectively selected as the Gudermannian function and the double exponential function. As a result, the integral sliding modes in these works have a more complex structure than (15) and contain the irrational number π. This is not conducive to the realization of the design of the sliding-mode surface. Therefore, our result extends the study in these references.

4.3 Reachability Analysis

In this subsection, the state $y_\ell(t)$ in (4) is successfully driven to the second-order SMS $\varrho_\ell(t) = 0$ and the SMS $\varpi_\ell(t) = 0$ at a predetermined moment by SOSM controller (19).

Calculate the derivative of $u_\ell(t)$ (19) as

$$\begin{aligned}\dot{u}_\ell(t) &= -B_\ell \dot{y}(t) - B_{d\ell}(1-\dot{d}(t))\dot{y}(t-d(t)) - \dot{\pounds}_\ell(t)\\ &\quad - \left(\frac{r_\ell - m_\ell}{\daleth_\ell^s m_\ell}|y_\ell(t)|^{-\frac{m_\ell}{r_\ell}} + \frac{1}{\daleth_\ell^s}\right)\dot{y}_\ell(t) F\left(y_\ell^{[\frac{m_\ell}{r_\ell}]}(t)\right)\\ &\quad - \left(\frac{108}{(\daleth_\ell^r)^2}\varpi_\ell^2(t) sign(\varrho_\ell(t)) + \delta_\ell sign(\varrho_\ell(t)) + \frac{2\pi}{\daleth_\ell^r}\left(\varrho_\ell^{[\frac{1}{2}]}(t)+\varrho_\ell^{[\frac{3}{2}]}(t)\right)^{[1]}\right).\end{aligned} \tag{25}$$

Also, the second-order derivative of $\varpi_\ell(t)$ in (15) is calculated to be

$$\begin{aligned}\ddot{\varpi}_\ell(t) &= B_\ell \dot{y}(t) + B_{d\ell}(1-\dot{d}(t))\dot{y}(t-d(t)) + \dot{\pounds}_\ell(t) + \dot{v}_\ell(t) + \dot{u}_\ell(t)\\ &\quad + \frac{r_\ell - m_\ell}{\daleth_\ell^s m_\ell}|y_\ell(t)|^{-\frac{m_\ell}{r_\ell}} \dot{y}_\ell(t) F\left(y_\ell^{[\frac{m_\ell}{r_\ell}]}(t)\right)\\ &\quad + \frac{1}{\daleth_\ell^s} y_\ell^{[1-\frac{m_\ell}{r_\ell}]}(t) y_\ell^{[\frac{m_\ell}{r_\ell}-1]}(t)\dot{y}_\ell(t) F\left(y_\ell^{[\frac{m_\ell}{r_\ell}]}(t)\right)\\ &= B_\ell \dot{y}(t) + B_{d\ell}(1-\dot{d}(t))\dot{y}(t-d(t)) + \dot{\pounds}_\ell(t) + \dot{v}_\ell(t) + \dot{u}_\ell(t)\\ &\quad + \left(\frac{r_\ell - m_\ell}{\daleth_\ell^s m_\ell}|y_\ell(t)|^{-\frac{m_\ell}{r_\ell}} + \frac{1}{\daleth_\ell^s}\right)\dot{y}_\ell(t) F\left(y_\ell^{[\frac{m_\ell}{r_\ell}]}(t)\right).\end{aligned} \tag{26}$$

Based on (18), we get the following upper-right derivative with respect to $\varrho_\ell(t)$:

$$D^+\varrho_\ell = \ddot{\varpi}_\ell(t) + \frac{1}{2\daleth_\ell^r}\frac{2(\daleth_\ell^r)^2|\dot{\varpi}_\ell(t)|\ddot{\varpi}_\ell(t) + 216\varpi_\ell^2(t)\dot{\varpi}_\ell(t)}{\left|(\daleth_\ell^r)^2\dot{\varpi}_\ell^{[2]}(t) + 72 sign(\varpi_\ell(t)) + 72\varpi_\ell^{[3]}(t)\right|^{\frac{1}{2}}}. \tag{27}$$

Theorem 3 *Suppose that Assumption 1 holds. For $\ell = 1, \ldots, p$, the track of state $y_\ell(t)$ of the closed-loop system (20) is successfully forced onto the relevant sliding manifolds $\varpi_\ell(t) = 0$ and $\dot{\varpi}_\ell(t) = 0$ in the period $\daleth_\ell^r$.*

Proof Construct the Lyapunov function below:

$$\mathscr{C}_1(t) = |\varrho_\ell(t)|.$$

The upper right-hand Dini derivative of $\mathscr{C}_1(t)$ for $\varrho_\ell(t) \neq 0$ is calculated as

$$\begin{aligned}D^+\mathscr{C}_1(t) &= \ddot{\varpi}_\ell(t) sign(\varrho_\ell(t))\\ &\quad + \frac{1}{2\daleth_\ell^r}\frac{2(\daleth_\ell^r)^2|\dot{\varpi}_\ell(t)|\ddot{\varpi}_\ell(t) sign(\varrho_\ell(t)) + 216\varpi_\ell^2(t)\dot{\varpi}_\ell(t) sign(\varrho_\ell(t))}{\left|(\daleth_\ell^r)^2\dot{\varpi}_\ell^{[2]}(t) + 72 sign(\varpi_\ell(t)) + 72\varpi_\ell^{[3]}(t)\right|^{\frac{1}{2}}}.\end{aligned}$$

Import $\dot{u}_\ell(t)$ (25) into (26) to obtain

$$\ddot{\varpi}_\ell(t) = -\frac{108}{(\daleth_\ell^r)^2}\varpi_\ell^2(t) sign(\varrho_\ell(t)) - \delta_\ell sign(\varrho_\ell(t)) - \frac{2\pi}{\daleth_\ell^r}\left(\varrho_\ell^{[\frac{1}{2}]}(t)+\varrho_\ell^{[\frac{3}{2}]}(t)\right)^{[1]}$$

$$+ \dot{v}_\ell(t).$$

Multiply the above equation by $sign(\varrho_\ell(t))$

$$\ddot{\varpi}_\ell(t) sign(\varrho_\ell(t)) = -\frac{108}{(\urcorner_\ell^r)^2}\varpi_\ell^2(t) - \delta_\ell - \frac{2\pi}{\urcorner_\ell^r}\bigg(|\varrho_\ell(t)|^{\frac{1}{2}} + |\varrho_\ell(t)|^{\frac{3}{2}}\bigg) + \dot{v}_\ell(t) sign(\varrho_\ell(t)).$$

Then, the following estimate for the derivative of the function $\mathscr{C}_1(t)$ is attained utilizing Assumption 1 and the above expression:

$$\begin{aligned} D^+\mathscr{C}_1(t) =& \ddot{\varpi}_\ell(t) sign(\varrho_\ell(t)) + \frac{1}{2\urcorner_\ell^r}\frac{-216|\dot{\varpi}_\ell(t)|\varpi_\ell^2(t)(1 - sign(\varrho_\ell(t)\dot{\varpi}_\ell(t)))}{\left|(\urcorner_\ell^r)^2\dot{\varpi}_\ell^{[2]}(t) + 72 sign(\varpi_\ell(t)) + 72\varpi_\ell^{[3]}(t)\right|^{\frac{1}{2}}} \\ &+ \frac{\pi}{2\urcorner_\ell^r}\frac{-4\urcorner_\ell^r|\dot{\varpi}_\ell(t)|\Big(|\varrho_\ell(t)|^{\frac{1}{2}} + |\varrho_\ell(t)|^{\frac{3}{2}}\Big)}{\left|(\urcorner_\ell^r)^2\dot{\varpi}_\ell^{[2]}(t) + 72 sign(\varpi_\ell(t)) + 72\varpi_\ell^{[3]}(t)\right|^{\frac{1}{2}}} \\ &+ \frac{1}{2\urcorner_\ell^r}\frac{-2(\urcorner_\ell^r)^2|\dot{\varpi}_\ell(t)|(\delta_\ell - \dot{v}_\ell(t) sign(\varrho_\ell(t)))}{\left|(\urcorner_\ell^r)^2\dot{\varpi}_\ell^{[2]}(t) + 72 sign(\varpi_\ell(t)) + 72\varpi_\ell^{[3]}(t)\right|^{\frac{1}{2}}} \\ \le& \ddot{\varpi}_\ell(t) sign(\varrho_\ell(t)) \\ \le& -\frac{2\pi}{\urcorner_\ell^r}\Big(\mathscr{C}_1^{\frac{1}{2}}(t) + \mathscr{C}_1^{\frac{3}{2}}(t)\Big). \end{aligned}$$

Use the notation $D^+\mathscr{C}_1(t) = \frac{d\mathscr{C}_1(t)}{dt}$ to convert the above expression to

$$\frac{d\mathscr{C}_1(t)}{\mathscr{C}_1^{\frac{1}{2}}(t) + \mathscr{C}_1^{\frac{3}{2}}(t)} \le -\frac{2\pi}{\urcorner_\ell^r}dt. \tag{28}$$

This is equivalent to

$$\frac{\mathscr{C}_1^{-\frac{1}{2}}(t)d\mathscr{C}_1(t)}{1 + \Big(\mathscr{C}_1^{\frac{1}{2}}(t)\Big)^2} \le -\frac{2\pi}{\urcorner_\ell^r}dt. \tag{29}$$

Introduce another new variable $\mathscr{E}_1(t) = \mathscr{C}_1^{\frac{1}{2}}(t)$ and calculate its derivative as $d\mathscr{E}_1(t) = \frac{1}{2}\mathscr{C}_1^{-\frac{1}{2}}(t)d\mathscr{C}_1(t)$. Then, using the variable substitution for (29), the following simple form can be obtained:

$$\frac{d\mathscr{E}_1(t)}{1 + \mathscr{E}_1^2(t)} \le -\frac{\pi}{\urcorner_\ell^r}dt. \tag{30}$$

Integrate each side of (30) from the initial time 0 to t

$$\int_0^t \frac{d\mathscr{E}_1(\curlywedge)}{1+\mathscr{E}_1^2(\curlywedge)} d\curlywedge \leq \int_0^t -\frac{\pi}{\daleth_\ell^r} d\curlywedge . \tag{31}$$

By (31), it's easy to deduce that

$$arctan\Big(|\varrho_\ell(t)|^{\frac{1}{2}}\Big) \leq arctan\Big(|\varrho_\ell(0)|^{\frac{1}{2}}\Big) - \frac{\pi}{\daleth_\ell^r} t.$$

From the above expression, it's simple to confirm that

$$\varrho_\ell(t) = 0$$

if and only if

$$arctan\Big(|\varrho_\ell(t)|^{\frac{1}{2}}\Big) = 0$$

is true. Therefore, we derive the settling-time function as

$$\daleth(\varrho_\ell(0)) = \frac{\daleth_\ell^r}{\pi} arctan\Big(|\varrho_\ell(0)|^{\frac{1}{2}}\Big). \tag{32}$$

Considering the fact that $0 \leq arctan\Big(|\varrho_\ell(0)|^{\frac{1}{2}}\Big) < \frac{\pi}{2}$, it follows that

$$\varrho_\ell(t) = 0, \quad \forall t \geq \frac{1}{2}\daleth_\ell^r.$$

This shows that the second-order SMS $\varrho_\ell(t) = 0$ is reachable in the predetermined period $\frac{1}{2}\daleth_\ell^r$.

When the trajectory of the system (4) reaches the second-order SMS $\varrho_\ell(t) = 0$, it can be seen that the following equation is true according to Eq. (18)

$$\dot{\varpi}_\ell(t) + \frac{1}{\daleth_\ell^r}\Big(\big(\daleth_\ell^r\big)^2 \dot{\varpi}_\ell^{[2]}(t) + 72 sign(\varpi_\ell(t)) + 72\varpi_\ell^{[3]}(t)\Big)^{[\frac{1}{2}]} = 0.$$

This is rewritten as

$$\dot{\varpi}_\ell(t) = -\frac{1}{\daleth_\ell^r}\Big((\daleth_\ell^r)^2 \dot{\varpi}_\ell^{[2]}(t) + 72 sign(\varpi_\ell(t)) + 72\varpi_\ell^{[3]}(t)\Big)^{[\frac{1}{2}]}. \tag{33}$$

From the properties $i)$ and $ii)$ (13), taking $(\cdot)^{[2]}$ on each side of (33) yields

$$(\dot{\varpi}_\ell(t))^{[2]} = -\frac{36}{\big(\daleth_\ell^r\big)^2}\Big(sign(\varpi_\ell(t)) + \varpi_\ell^{[3]}(t)\Big). \tag{34}$$

Taking $(\cdot)^{[\frac{1}{2}]}$ on both sides of (34) leads to

$$\dot{\varpi}_\ell(t) = -\frac{6}{\daleth_\ell^r}\Big(sign(\varpi_\ell(t)) + \varpi_\ell^{[3]}(t)\Big)^{[\frac{1}{2}]}. \tag{35}$$

The Lyapunov function candidate is selected below:

$$\mathscr{C}_1(t) = |\varpi_\ell(t)|.$$

Derive the upper right-hand Dini derivative of $\mathscr{C}_1(t)$ following the state track of (35) to be

$$\begin{aligned} D^+\mathscr{C}_1(t) &= \dot{\varpi}_\ell(t)sign(\varpi_\ell(t)) \\ &= -\frac{6}{\daleth_\ell^r}\Big(1 + |\varpi_\ell(t)|^3\Big)^{\frac{1}{2}} \\ &= -\frac{6}{\daleth_\ell^r}\Big(1 + \mathscr{C}_1^3(t)\Big)^{\frac{1}{2}}. \end{aligned}$$

Assuming that γ_1^r is the arrival period for the second-order SMS $\varrho_\ell(t) = 0$, one knows: $|\varpi_\ell(t)| = 0$ for all $t \geq \daleth_\ell^r \geq \gamma_1^r + \frac{2}{6}\daleth_\ell^r + \frac{1}{6}\daleth_\ell^r$ and any solution $\varpi_\ell(t)$ of (35) in accordance with Theorem 1. Naturally, the following is true according to (35):

$$\dot{\varpi}_\ell(t) = 0, \ \forall t \geq \daleth_\ell^r.$$

As a result, the fixed-time stability at the moment $\daleth_\ell^r$ for sliding mode surfaces $\varpi_\ell(t) = 0$ and $\dot{\varpi}_\ell(t) = 0$ could be realized. The evidence is finished. □

Remark 6 Consider the equation $\tilde{\varrho}_\ell(t) = \dot{\varpi}_\ell(t) + \frac{1}{\daleth_\ell^r}\Big(\big(\daleth_\ell^r\big)^2\dot{\varpi}_\ell^{[2]}(t) + 72 sign(\varpi_\ell(t))\Big)^{[\frac{1}{2}]}$. Then, the state trajectories of the equations $\tilde{\varrho}_\ell(t) = 0$ and $\varrho_\ell(t) = 0$, respectively, confirm the finite-time and fixed-time reachability of the SMS (15) (Fig. 3 displays the details). On the other hand, the new polynomial, $\varrho_\ell^{[\frac{3}{2}]}(t)$, is crucial in ensuring the reachability in a fixed time for the sliding manifold (18).

Theorem 4 *If Assumption 1 holds, then the global stability of the nonlinear system (1) is accomplished at a fixed period through controller (19). Furthermore, an upper bound on the estimated settling period is*

$$\daleth_{max} = max\left\{\daleth_\ell^r\right\} + max\left\{\daleth_\ell^s\right\}, \tag{36}$$

where $\ell = 1, \ldots, p$.

Proof For $l = 1, 2, \ldots, p$, the global stability of system (4) at the moment $\daleth_\ell^r + \daleth_\ell^s$ can be verified from Theorems 2 and 3, namely, the system (4) is globally stable at a fixed time under controller (19). Therefore, the global stability of system (1) could be realized at the settling period $\daleth_{max}$. The evidence is finished. □

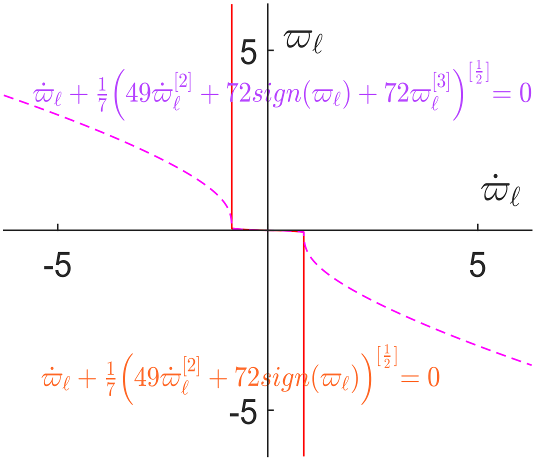

Fig. 3 The finite-time and fixed-time reachability for the sliding manifold (15) when $\daleth_\ell^r = 7$

To clearly reflect the second-order SMC for system (1), the SOSMCA is developed below:

Algorithm 1 ▶ Step 1. From the actual demand, the positive δ_ℓ satisfing Assumption 1, positive integers r_ℓ and m_ℓ satisfing $0 < \frac{m_\ell}{r_\ell} < 1$, and positive $\daleth_\ell^s$ and $\daleth_\ell^r$ are selected.
▶ Step 2. Produce the SMC law according to equations (15), (18), and (19).
▶ Step 3. Apply the generated SMC law to the nonlinear system (4).

Next, using the specialization of the aforementioned control scheme, the stability of nonlinear systems without time delays and linear systems with time delays at a fixed time is determined.
The nonlinear system without time delays is described as follows in this article:

$$\begin{aligned} \dot{y}(t) =& By(t) + \pounds(t, y(t)) + v(t) + u(t), \\ y(0) =& \varkappa, \end{aligned} \tag{37}$$

in which $y(t) \in \Re^p$ denotes the system's state. $B \in \Re^{p\times p}$ denotes the constant matrix. $\pounds(\cdot) \in \Re^p$ represents the non-linear function. $v(t) \in \Re^p$ represents the uncertain disturbance. $u(t) \in \Re^p$ denotes the input signal. $\varkappa$ corresponds to the initial value of the system.

Corollary 1 *If Assumption 1 holds, then the following sliding mode controller can stabilize the nonlinear system (37) within a fixed time* $\daleth_{max} = max_\ell \left\{\daleth^r_\ell\right\} + max_\ell \left\{\daleth^s_\ell\right\}$,

$$\begin{aligned} u_\ell(t) = & -B_\ell y(t) - \pounds_\ell(t) - \frac{r_\ell}{\daleth^s_\ell m_\ell} y_\ell^{[1-\frac{m_\ell}{r_\ell}]}(t) F\Big(y_\ell^{[\frac{m_\ell}{r_\ell}]}(t)\Big) \\ & - \int_0^t \Bigg(\frac{108}{(\daleth^r_\ell)^2}\varpi^2_\ell(\curlywedge) sign(\varrho_\ell(\curlywedge)) + \delta_\ell sign(\varrho_\ell(\curlywedge)) \\ & + \frac{2\pi}{\daleth^r_\ell}\Big(\varrho_\ell^{[\frac{1}{2}]}(\curlywedge) + \varrho_\ell^{[\frac{3}{2}]}(\curlywedge)\Big)^{[1]}\Bigg) d\curlywedge \end{aligned} \tag{38}$$

where $\ell = 1, \ldots, p$. B_ℓ *represents the* ℓth *row of the matrix* B. $y_\ell(t)$, $\pounds_\ell(t)$, as well as $u_\ell(t)$, *respectively, represent the* ℓth *element in vectors* $y(t)$, $\pounds(t)$, *and* $u(t)$. *The sliding mode surface (SMS) and the second-order SMS, respectively, are*

$$\varpi_\ell(t) = y_\ell(t) + \frac{r_\ell}{\daleth^s_\ell m_\ell}\int_0^t y_\ell^{[1-\frac{m_\ell}{r_\ell}]}(\curlywedge) F\Big(y_\ell^{[\frac{m_\ell}{r_\ell}]}(\curlywedge)\Big) d\curlywedge \tag{39}$$

and

$$\varrho_\ell(t) = \dot{\varpi}_\ell(t) + \frac{1}{\daleth^r_\ell}\Big((\daleth^r_\ell)^2 \dot{\varpi}_\ell^{[2]}(t) + 72 sign(\varpi_\ell(t)) + 72\varpi_\ell^{[3]}(t)\Big)^{[\frac{1}{2}]}. \tag{40}$$

Additionally, take into account the following linear system with time delays in this article:

$$\begin{aligned} \dot{y}(t) = & By(t) + B_d y(t - d(t)) + v(t) + u(t), \\ y(t) = & \varkappa(t), \quad \forall t \in [-\hbar, 0], \end{aligned} \tag{41}$$

in which all of the above symbols are defined in the same way as in system (1).

Corollary 2 *If Assumption 1 is satisfied, then the sliding mode controller shown below could stabilize the nonlinear system (41) within a fixed time* $\daleth_{max} = max_\ell \left\{\daleth^r_\ell\right\} + max_\ell \left\{\daleth^s_\ell\right\}$,

$$\begin{aligned} u_\ell(t) = & -B_\ell y(t) - B_{d\ell} y(t - d(t)) - \frac{r_\ell}{\daleth^s_\ell m_\ell} y_\ell^{[1-\frac{m_\ell}{r_\ell}]}(t) F\Big(y_\ell^{[\frac{m_\ell}{r_\ell}]}(t)\Big) \\ & - \int_0^t \Bigg(\frac{108}{(\daleth^r_\ell)^2}\varpi^2_\ell(\curlywedge) sign(\varrho_\ell(\curlywedge)) + \delta_\ell sign(\varrho_\ell(\curlywedge)) \\ & + \frac{2\pi}{\daleth^r_\ell}\Big(\varrho_\ell^{[\frac{1}{2}]}(\curlywedge) + \varrho_\ell^{[\frac{3}{2}]}(\curlywedge)\Big)^{[1]}\Bigg) d\curlywedge \end{aligned} \tag{42}$$

where $\ell = 1, \ldots, p$. B_ℓ *and* $B_{d\ell}$ *denote the* ℓth *row of matrices* B and B_d, *respectively.* $y_\ell(t)$ as well as $u_\ell(t)$, *respectively, represent the* ℓth *element in* $y(t)$ *and* $u(t)$. *The* *sliding mode surface (SMS)*

$$\varpi_\ell(t) = y_\ell(t) + \frac{r_\ell}{\daleth^s_\ell m_\ell}\int_0^t y_\ell^{[1-\frac{m_\ell}{r_\ell}]}(\curlywedge)F\Big(y_\ell^{[\frac{m_\ell}{r_\ell}]}(\curlywedge)\Big)d\curlywedge. \tag{43}$$

The second-order SMS

$$\varrho_\ell(t) = \dot{\varpi}_\ell(t) + \frac{1}{\daleth^r_\ell}\Big((\daleth^r_\ell)^2\dot{\varpi}_\ell^{[2]}(t) + 72sign(\varpi_\ell(t)) + 72\varpi_\ell^{[3]}(t)\Big)^{[\frac{1}{2}]}. \tag{44}$$

Remark 7 The advantage of the proposed sliding variable (15) and second-order SMS (18) is that the real predetermined convergence period is a standalone construction value. It is directly displayed in the sliding mode equations as the sum of $\daleth^s_\ell$ and $\daleth^r_\ell$. This allows us to adjust the setting time in advance based on performance requirements and, particularly, in the most apparent manner. In addition, every sliding-mode variable has an independent settling period. This property makes it possible for the setting period of the selected state in the closed-loop system to be adjusted without dependence on other states.

Remark 8 Be aware that the SOSM controller (19) reduces the chattering phenomenon to some extent but does not completely eliminate it. This is because the sign function adopted in controllers inevitably introduces the chattering phenomenon to control signals, and the system states [14, 23, 39, 54]. To solve this issue, the authors try to generate a suitable continuous control from the discontinuous control [1, 27]. One typical method is to substitute $\frac{y_\ell(t)}{|y_\ell(t)|+\eta}$ for $sign(y_\ell(t))$, in which $\eta > 0$ represents a tiny constant. In this manner, the robustness of the SOSM control is going to be impacted.

5 Simulation

The subsequent numerical experiment is utilized to examine the efficacy of the suggested SMC technique. The SMC problem for the specified nonlinear system is what we are trying to verify.

Example 1 Take into account the system (1), in which the matrix B is derived from the widely used F-404 airplane's engine system [20]

$$B = \begin{bmatrix} -1.46 & 0 & 2.428 \\ 0.1643 & -0.4 & -0.3788 \\ 0.3107 & 0 & -2.23 \end{bmatrix},$$

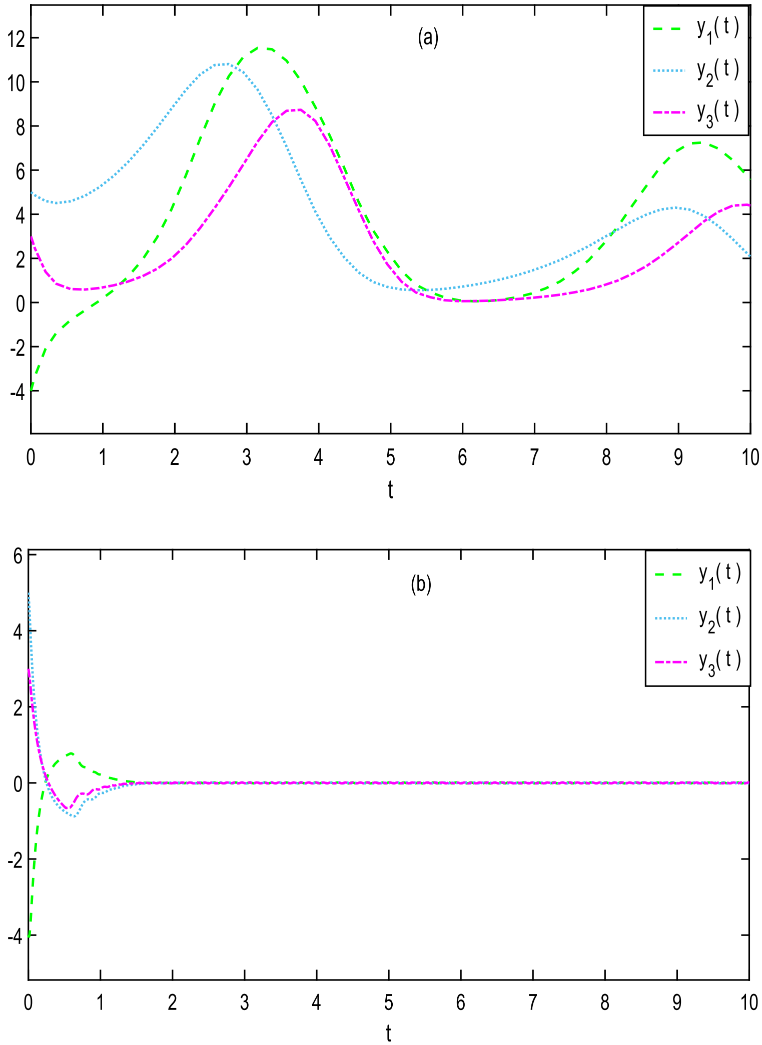

Fig. 4 The tracks of system (1) without as well as with the controller (19)

and the other parameters for the system are set as

$$B_d = \begin{bmatrix} -0.1 & 0 & 0.2 \\ 0.1 & -0.01 & -0.03 \\ 0.04 & 0.5 & -0.3 \end{bmatrix},$$

$$\pounds(t) = \begin{bmatrix} sin(t)(y_1(t) + y_1(t-d(t))) \\ \frac{1}{2}sin(t)(y_2(t) + y_2(t-d(t))) \\ cos(t)(y_3(t) + y_3(t-d(t))) \end{bmatrix}, v(t) = \begin{bmatrix} sin(t) \\ cos(t) \\ \frac{1}{2}sin(t) \end{bmatrix},$$

$$d(t) = 0.1 + 0.1sin(t^2), \hbar = 0.2.$$

It should be noted that, when the matrix B_d equals the matrix 0, the system (1) as defined above becomes a class of the F-404 airplane's engine system in [20]. As shown in the meaning of symbols in the formula (1), details related to the F-404 airplane's engine system can be obtained from it, such as inputs, outputs, and measurements. Additionally, it's worth pointing out that $d(t)$ is bounded, but the derivative of $d(t)$ is unbounded. Next, we design a SOSM controller based on Algorithm 1 to stabilize the above nonlinear system. Given the performance parameters $\urcorner_1^s = \urcorner_2^s = \urcorner_3^s = 2,\ \urcorner_1^r = \urcorner_2^r = \urcorner_3^r = 2,\ r_1 = r_2 = r_3 = 2,\ m_1 = m_2 = m_3 = 1,\ \delta_1 = \delta_2 = 1,$ and $\delta_3 = \frac{1}{2}$, the SMS function (15) and the second-order SMS (18) are, respectively, computed as

$$\varpi_\ell(t) = y_\ell(t) + \int_0^t y_\ell^{[\frac{1}{2}]}(\curlywedge) F\left(y_\ell^{[\frac{1}{2}]}(\curlywedge)\right) d\curlywedge,$$

$$\varrho_\ell = \dot{\varpi}_\ell(t) + \frac{1}{2}\left(4\dot{\varpi}_\ell^{[2]}(t) + 72 sign(\varpi_\ell(t)) + 72\varpi_\ell^{[3]}(t)\right)^{[\frac{1}{2}]}.$$

As a result, the intended SOSM controller (19) could be derived as follows:

$$\begin{cases} \dot{u}_1(t) = 1.46y_1(t) - 2.4283y_3(t) + 0.1y_1(t-d(t)) - 0.2y_3(t-d(t)) - sin(t)(y_1(t) + y_1(t-d(t))) \\ \quad - y_1^{[\frac{1}{2}]}(t)F\left(y_1^{[\frac{1}{2}]}(t)\right) - \int_0^t \left(27\varpi_1^2(\curlywedge)sign(\varrho_1(\curlywedge)) + sign(\varrho_1(\curlywedge)) \right. \\ \quad \left. + \pi\left(\varrho_1^{[\frac{1}{2}]}(\curlywedge) + \varrho_1^{[\frac{3}{2}]}(\curlywedge)\right)^{[1]}\right) d\curlywedge, \\ \dot{u}_2(t) = -0.1643y_1(t) + 0.4y_2(t) + 0.3788y_3(t) - 0.1y_1(t-d(t)) + 0.01y_2(t-d(t)) + 0.03y_3(t-d(t)) \\ \quad - \frac{1}{2}sin(t)(y_2(t) + y_2(t-d(t))) \\ \quad - y_2^{[\frac{1}{2}]}(t)F\left(y_2^{[\frac{1}{2}]}(t)\right) - \int_0^t \left(27\varpi_2^2(\curlywedge)sign(\varrho_2(\curlywedge)) + sign(\varrho_2(\curlywedge)) \right. \\ \quad \left. + \pi\left(\varrho_2^{[\frac{1}{2}]}(\curlywedge) + \varrho_2^{[\frac{3}{2}]}(\curlywedge)\right)^{[1]}\right) d\curlywedge, \\ \dot{u}_3(t) = -0.3107y_1(t) + 2.23y_3(t) - 0.04y_1(t-d(t)) - 0.5y_2(t-d(t)) + 0.3y_3(t-d(t)) \\ \quad - cos(t)(y_3(t) + y_3(t-d(t))) \\ \quad - y_3^{[\frac{1}{2}]}(t)F\left(y_3^{[\frac{1}{2}]}(t)\right) - \int_0^t \left(27\varpi_3^2(\curlywedge)sign(\varrho_3(\curlywedge)) + \frac{1}{2}sign(\varrho_3(\curlywedge)) \right. \\ \quad \left. + \pi\left(\varrho_3^{[\frac{1}{2}]}(\curlywedge) + \sigma_3^{[\frac{3}{2}]}(\curlywedge)\right)^{[1]}\right) d\curlywedge. \end{cases} \tag{45}$$

According to Theorem 4, the global fixed-time stability of the nonlinear system (1) is realized through controller (19), where the initial value is assumed as $y(0) = [-4\ \ 5\ \ 3]^T$ and the estimated predetermined period is calculated to be $\urcorner_{max} = 4$.

To display the viability of the suggested SMC technique, simulation outcomes are provided in Figs. 4, 5, 6 and 7. Figure 4 depicts the states $y(t)$ of the system (1) without as well as with a controller. Figures 5, 6 and 7, respectively, display the derivative of the SMS function (15), the SMS function (15) and the second-order

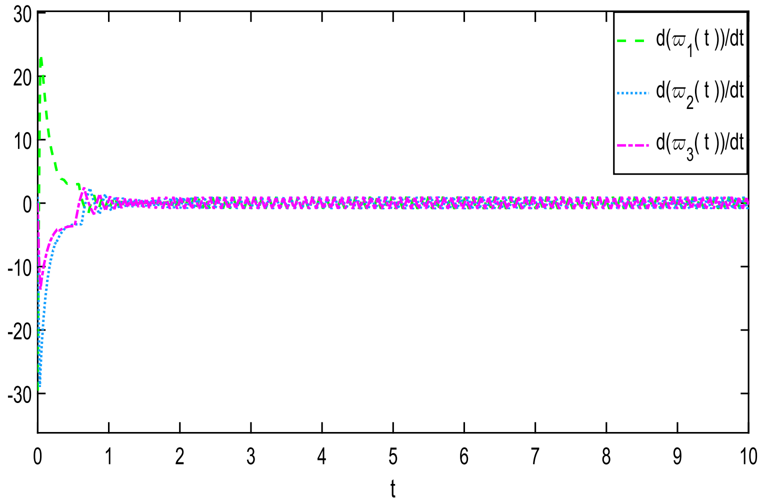

Fig. 5 The derivative of the SMS function (15)

SMS (18), and the SOSM controller (19). It is apparent that the nonlinear system (1) with disturbances is stabilized by the controller (19) within 2 time units before $\daleth_{max} = max\left\{\daleth_{\ell}^{r}\right\} + max\left\{\daleth_{\ell}^{s}\right\} = 4$, which is demonstrated in Fig. 4a, b. In addition, Fig. 7 shows that the chattering of the control signal (19) is slight. Therefore, the simulation results validate the advantages and limitations of the proposed control scheme, as indicated in Remarks 7 and 8.

6 Conclusion

In this paper, the second-order SMC theory is successfully extended for the first time to accomplish the stability of a class of nonlinear systems in a fixed time. In this process, novel sliding module surfaces and an improved result for stability are developed to realize the stability and reachability of the sliding module in a fixed period. The outstanding advantage of the SOSMCA obtained in this article is that it reduces the tremor phenomenon. Considering that the tremor has not been completely eliminated, we will extend this control algorithm to neural sliding mode control to remedy this deficiency in the future. As is known to all, the integrator proposed in neural sliding mode control can filter the high-frequency switch generated by SMC.

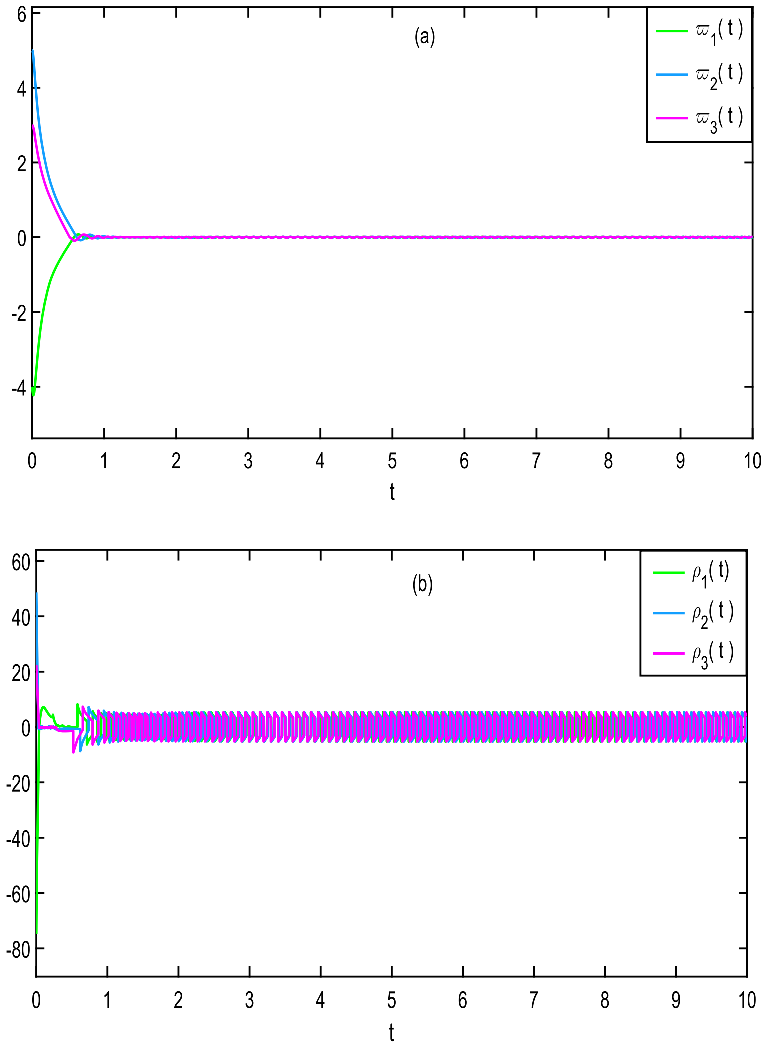

Fig. 6 The SMS function (15) and the second-order SMS (18)

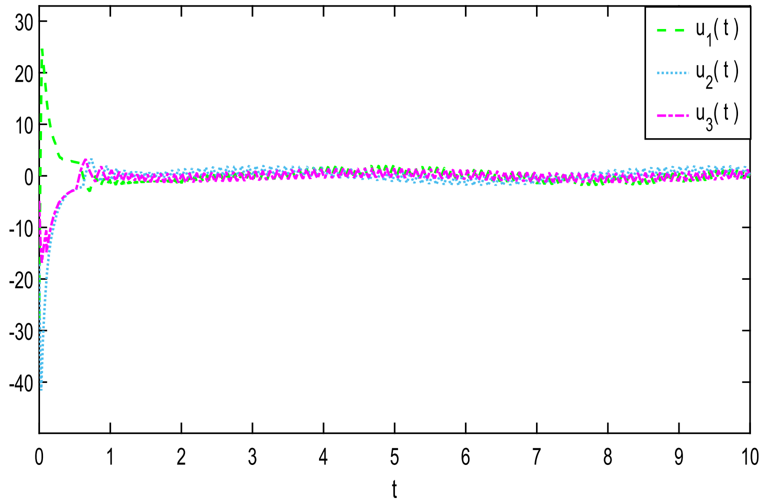

Fig. 7 The SOSM controller (19)

Acknowledgements This research was partially funded by the National Natural Science Foundation of China (62373383), the Fundamental Research Funds for the Central Universities (CZT20020), and the Academic Team in Universities (KTZ20051).

Data Availability This paper does not engage in data sharing because no datasets were created or evaluated for the present research.

Declarations

Conflict of interest The authors affirm their claim to not have any conflict of interest.

References

1. G. Ambrosino, G. Celektano, F. Garofalo, Variable structure model reference adaptive control systems. Int. J. Control **39**(6), 1339–1349 (1984)
2. L. Arie, Sliding order and sliding accuracy in sliding mode control. Int. J. Control **58**(6), 1247–1263 (1993)
3. Q. Chen, D. Tong, W. Zhou, Y. Xu, Adaptive exponential state estimation for Markovian jumping neural networks with multi-delays and Levy noises. Circuits Syst. Signal Process. **38**(7), 3321–3339 (2019)
4. S. Ding, S. Li, Second-order sliding mode controller design subject to mismatched term. Automatica **77**, 388–392 (2017)
5. S. Ding, J.H. Park, C.C. Chen, Second-order sliding mode controller design with output constraint. Automatica **112**, 108704 (2020)
6. R. Errouissi, J. Yang, W.H. Chen, A.D. Ahmed, Robust nonlinear generalised predictive control for a class of uncertain nonlinear systems via an integral sliding mode approach. Int. J. Control **89**(8), 1698–1710 (2016)
7. M. Forti, M. Grazzini, P. Nistri, Generalized Lyapunov approach for convergence of neural networks with discontinuous or non-Lipschitz activations. Phys. D Nonlinear Phenom. **214**, 88–99 (2006)

8. J.P. Gauthier, H. Hammouri, S. Othman, A simple observer for nonlinear systems applications to bioreactors. IEEE Trans. Autom. Control **37**(6), 875–880 (1992)
9. K. Gu, J. Chen, V.L. Kharitonov, *Stability of Time-Delay Systems* (Springer, Berlin, 2003)
10. V.V. Huynh, New observer-based control design for mismatched uncertain systems with time-delay. Arch. Control Sci. **26**(4), 597–610 (2016)
11. S. Jiang, X. Lu, G. Cai, S. Cai, Adaptive fixed-time control for cluster synchronisation of coupled complex networks with uncertain disturbances. Int. J. Syst. Sci. **48**, 1–9 (2017)
12. M. Jouini, S. Dhahri, A. Sellami, Combination of integral sliding mode control design with optimal feedback control for nonlinear uncertain systems. Trans. Inst. Meas. Control **41**(5), 1331–1339 (2019)
13. A. Khanzadeh, I. Mohammadzaman, Fixed-time integral sliding mode control design for a class of uncertain nonlinear systems based on a novel fixed-time stability condition. Eur. J. Control **69**, 100753 (2023)
14. A. Khanzadeh, M. Pourgholi, Fixed-time sliding mode controller design for synchronization of complex dynamical networks. Nonlinear. Dyn. **88**(4), 2637–2649 (2017)
15. S. Laghrouche, F. Plestan, A. Glumineau, Higher order sliding mode control based on integral sliding mode. Automatica **43**(3), 531–537 (2007)
16. H. Li, J. Wang, L. Wu, H.K. Lam, Y. Gao, Optimal guaranteed cost sliding-mode control of interval type-2 fuzzy time-delay systems. IEEE Trans. Fuzzy Syst. **26**(1), 246–257 (2018)
17. X. Liao, L. Wang, P. Yu, *Stability of Dynamical Systems*, vol. 5 (Elsevier, Amsterdam, 2007)
18. Y.H. Liu, H. Li, Q.S. Zhong, S.M. Zhong, Finite-time control for uncertain systems with nonlinear perturbations. Adv. Differ. Equ. **2017**(1), 1–28 (2017)
19. L. Liu, S.H. Ding, A unified control approach to finite-time stabilization of SOSM dynamics subject to an output constraint. Appl. Math. Comput. **394**, 125752 (2021)
20. M. Liu, L. Zhang, P. Shi, Y. Zhao, Fault estimation sliding mode observer with digital communication constraints. IEEE Trans. Autom. Control **63**(10), 3434–3441 (2018)
21. A. Michalak, Finite-time and fixed-time stability analysis for time-varying systems: a dual approach. J. Frankl. Inst. **359**(18), 10676–10687 (2022)
22. S. Mondal, C. Mahanta, Chattering free adaptive multivariable sliding mode controller for systems with matched and mismatched uncertainty. ISA Trans. **52**(3), 335–341 (2013)
23. B.B. Musmade, B.M. Patre, Robust sliding mode control of uncertain nonlinear systems with chattering alleviating scheme. Int. J. Mod. Phys. B **35**(14), 66 (2021)
24. A. Polyakov, Fixed-time stabilization via second order sliding mode control. IFAC Proc. **45**(9), 254–258 (2012)
25. A.L. Shang, W.J. Gu, Model-following adaptive second-order sliding model control of a class of nonlinear uncertain systems, in *Conference: International Symposium on Instrumentation and Control Technology* (2003)
26. W.C. Sun, Y.Q. Yuan, Passivity based hierarchical multi-task tracking control for redundant manipulators with uncertainties. Automatica **155**, 2023 (2023)
27. D.B. Tong, C. Xua, Q.Y. Chen, W.N. Zhou, Sliding mode control of a class of nonlinear systems. J. Frankl. Inst. **357**(3), 1560–1581 (2020)
28. D. Tong, Q. Chen, W. Zhou, J. Zhou, Y. Xu, Multi-delay-dependent exponential synchronization for neutral-type stochastic complex networks with Markovian jump parameters via adaptive control. Neural Process. Lett. **49**(3), 1611–1628 (2018)
29. D. Tong, P. Rao, Q. Chen, M.J. Ogorzalek, X. Li, Exponential synchronization and phase locking of a multilayer Kuramoto-oscillator system with a pacemaker. Neurocomputing **308**, 129–137 (2018)
30. D. Tong, L. Zhang, W. Zhou, J. Zhou, Y. Xu, Asymptotical synchronization for delayed stochastic neural networks with uncertainty via adaptive control. Int. J. Control Autom. Syst. **14**(3), 706–712 (2016)
31. X.T. Tran, H. Oh, A modified generic second order algorithm with fixed-time stability. ISA Trans. (2020). https://doi.org/10.1016/j.isatra.2020.10.021
32. V.I. Utkin, *Sliding Mode in Control and Optimization* (Springer, Berlin, 1992)
33. M. Vidyasagar, *Nonlinear Systems Analysis*, vol. 42 (SIAM, Philadelphia, 2002)
34. Z.B. Wang, H.Q. Wu, Projective synchronization in fixed time for complex dynamical networks with nonidentical nodes via second-order sliding mode control strategy. J. Frankl. Inst. (2019). https://doi.org/10.1016/j.jfranklin.2018.07.018
35. J. Wang, X.M. Zhang, Q.L. Han, Event-triggered generalized dissipativity filtering for neural networks with time-varying delays. IEEE Trans. Neural Netw. Learn. Syst. **27**(1), 77–88 (2015)

36. C.X. Wang, Y.Q. Wu, Finite-time tracking control for strict-feedback nonlinear systems with full state constraints. Int. J. Control **92**(6), 1426–1433 (2019)
37. Y. Wang, H.R. Karimi, H. Shen, Z. Fang, M. Liu, Fuzzy-model-based sliding mode control of nonlinear descriptor systems. IEEE. Trans. Cybern. **49**(9), 3409–3419 (2019)
38. Y.Y. Wang, Y.Q. Xia, H.Y. Li, P.F. Zhou, A new integral sliding mode design method for nonlinear stochastic systems. Automatica **90**, 304–309 (2018)
39. J. Wu, X.F. Wang, R.R. Ma, X.H. Pang, L. Zhao, Chattering analysis on finite/fixed-time consensus of multi-agent systems. J. Chin. Inst. Eng. **45**(1), 17–26 (2022)
40. J. Xia, J. Zhang, W. Sun, B. Zhang, Z. Wang, Finite-time adaptive fuzzy control for nonlinear systems with full state constraints. IEEE Trans. Syst. Man Cybern. Syst. **49**(7), 1541–1548 (2019)
41. Q.Z. Xiao, H.L. Liu, Z.H. Xu, Z.G. Yang, On collision avoiding fixed-time flocking with measurable diameter to a Cucker–Smale-type self-propelled particle model. Complexity **2020**, 1–12 (2020)
42. B. Xu, Composite learning finite-time control with application to quadrotors. IEEE Trans. Syst. Man Cybern. Syst. **13**(99), 1–10 (2017)
43. C. Xu, D. Tong, Q. Chen, W. Zhou, P. Shi, Exponential stability of Markovian jumping systems via adaptive sliding mode control. IEEE Trans. Syst. Man Cybern. Syst. **51**(2), 1–11 (2019)
44. D.H. Zhang, Y.L. Si, Z. Chen, A coupled numerical framework for hybrid floating offshore wind turbine and oscillating water column wave energy converters. Energy Convers. Manag. **267**, 2022 (2022)
45. J. Zhang, J.W. Xia, W. Sun, G. Zhuang, Z. Wang, Finite-time tracking control for stochastic nonlinear systems with full state constraints. Appl. Math. Comput. **338**, 207–220 (2018)
46. B.L. Zhang, Q. Han, X. Zhang, X. Yu, Sliding mode control with mixed current and delayed states for offshore steel jacket platforms. IEEE Trans. Control Syst. Technol. **22**(5), 1769–1783 (2014)
47. X.L. Zhang, Y. Yi, X. Guang, Event-triggered integral sliding mode anti-disturbance control for non-linear systems via T-S disturbance modeling. IEEE Access **9**, 1855–1863 (2021)
48. X.Y. Zhang, SMC for nonlinear systems with mismatched uncertainty using Lyapunov-function integral sliding mode. Int. J. Control **95**(10), 2710–2725 (2022)
49. X.Y. Zhang, X.D. Li, J.D. Cao, F. Miaadi, Design of memory controllers for finite-time stabilization of delayed neural networks with uncertainty. J. Frankl. Inst. **355**(13), 5394–5413 (2018)
50. H. Zhao, L. Li, H. Peng, J. Xiao, Y. Yang, M. Zheng, Fixed-time synchronization of multi-links complex network. Mod. Phys. Lett. B **31**(2), 1–24 (2017)
51. B.C. Zheng, J.H. Park, Sliding mode control design for linear systems subject to quantization parameter mismatch. J. Frankl. Inst. **353**(1), 37–53 (2016)
52. L. Zhou, J. She, X. Zhang, Z. Cao, Z. Zhang, Performance enhancement of repetitive-control systems and application to tracking control of chuck-workpiece systems. IEEE Trans. Ind. Electron. (2019). https://doi.org/10.1109/TIE.2019.2921272
53. L. Zhou, J. She, S. Zhou, Robust H∞ control of an observer-based repetitive-control system. J. Frankl. Inst. **355**(12), 4952–4969 (2018)
54. Y. Zhou, C. Sun, Fixed time synchronization of complex dynamical networks, in *Proceedings of the 2015 Chinese Intelligent Automation Conference, Wuhan, China* (2015), pp. 163–170
55. Z.Y. Zuo, T. Lin, Distributed robust finite-time nonlinear consensus protocols for multi-agent systems. Int. J. Syst. Sci. **47**(6), 1366–1375 (2014)